Lipid Transfer between Small Unilamellar Vesicles and Single Bilayers on a Solid Support: Self-Assembly of Supported Bilayers with Asymmetric Lipid Distribution†

Herbert M. Reinl and Thomas M. Bayerl*

Technische Universität München, Physik Department E22, D85748 Garching, Germany

Received May 17, 1994; Revised Manuscript Received September 14, 1994®

ABSTRACT: The transfer of lipids between small unilamellar vesicles of either dimyristoylphosphatidylcholine (DMPC), dimyristoylphosphatidylglycerol (DMPG), or dioctadecyl diammonium bromide (DODAB) and a single bilayer on a solid support of chain perdeuterated DMPC-d_{54} has been studied by time-resolved ATR infrared spectroscopy, deuterium NMR, and DSC. The IR method was used for measuring the transfer kinetics and the amount of lipid transferred to the supported bilayer, while NMR was employed for the assessment of molecular order and for the occurrence of lipid asymmetries due to the transfer. We find that the composition of a supported planar dimyristoylphosphatidylcholine (DMPC-d_{54}) bilayer can be modified by incubation with high concentrations of sonicated vesicles consisting of the donor lipid. Three cases were studied. First, the incubation was done with DMPC as donor lipid. The kinetics of this process is double exponential and comparatively slow, with a half-time in the range of several hours. The activation energy was estimated as 50 ± 2 kJ/mol. In a second set of measurements, cationic DODAB or anionic DMPG was used as donor lipid. The kinetics of this transfer is 1 order of magnitude faster than for DMPC and can be described by a single exponential. For DMPG transfer, we obtained an activation energy of 35 ± 2 kJ/mol. Independent of the headgroup charge of the donor lipid, 25−35% of the (acceptor) DMPC in the supported bilayer is not accessible for exchange with the donor lipid. The transfer of either DMPG or DODAB causes drastic changes of the phase transition behavior of the supported bilayer without significantly altering the lipid packing density of the lipids. In a third set of experiments, the supported bilayer was subjected to a sequential transfer of DMPG and DODAB. We find significant differences in the final supported bilayer composition and packing density depending on whether DODAB or DMPG is transferred first. Deuterium NMR indicates that such sequential lipid transfer gives rise to an asymmetric lipid distribution between the two monolayers of the supported bilayer.

Lipid transfer between bilayers is a well-known phenomenon and has been studied in detail by various methods (Brown, 1992). For bilayer vesicles, the process appears to occur mainly via diffusion of lipid monomers through the aqueous medium but may involve a more efficient direct transfer due to vesicle collisions at higher concentrations (Jones & Thompson, 1990, 1989; Wimley & Thompson, 1991).

Phospholipid bilayers on a solid support provide a new, geometrically well-defined model system with interesting applications in membrane studies using fluorescence (Tamm & McConnell, 1985; Thompson & Palmer, 1988), infrared spectroscopy (Tamm & Tatulian, 1993; Frey & Tamm, 1991; Reinl & Bayerl, 1993), NMR (Dolainsky et al., 1993; Köchy & Bayerl, 1993), calorimetry (Naumann et al., 1992), and neutron scattering (Johnson et al., 1991). Despite this wide field of application, little is known about the lipid transfer between supported bilayers or between supported bilayers and vesicles. It has been demonstrated recently by DSC measurements (Naumann et al., 1992) that lipid transfer between single bilayers on a spherical support has some features similar to those observed for transfer between sonicated vesicles (Bayerl et al., 1988) but is significantly slower. This could be caused by the inhibition of collisions in the supported systems compared to free vesicles. The attractive potential that keeps the bilayer adsorbed to the solid surface may also contribute to a slowdown of transfer by increasing the activation energy for the desorption of lipid monomers from the supported bilayer.

Lipid bilayers on a solid support can be prepared either by the well-established Langmuir−Blodgett techniques or by a process of solid surface induced fusion of sonicated vesicles (Iler, 1979; McConnell et al., 1986; Czaja et al., 1987). The latter process is not fully understood yet, but the underlying molecular processes could be similar to those for lipid transfer between sonicated vesicles and a supported bilayer.

A further intriguing question is the possible formation of asymmetric supported bilayers by lipid transfer involving electrically charged lipids. Considering that the solid support itself exhibits a negative surface charge (e.g., for silica or silicon), it is conceivable that anionic lipids are depleted in the monolayer leaflet facing the support. This question is also interesting from a biological point of view: For example, the erythrocyte membrane is supported by a cytoskeleton consisting of proteins with an excess electric charge. So far, there is no convincing experimental evidence that the presence of a charged surface supporting a bilayer may induce an asymmetry of its transverse lipid distribution.

† This work was supported by a grant from the Hertie Stiftung and by the Sonderforschungsbereich 266 of the Deutsche Forschungsgemeinschaft.

* Address correspondence to this author; Phone: 011 49 89 3209 2480; Fax: 011 49 89 3209 2469; e-mail address: tbayerl@physik.tu-muenchen.de.

® Abstract published in *Advance ACS Abstracts,* October 15, 1994.

0006-2960/94/0433-14091$04.50/0

Attenuated total reflection (ATR) infrared measurements on lipid bilayers are well-established for obtaining structural information and for protein−lipid interaction studies (Tamm & Tatulian, 1993; Frey & Tamm, 1991; Okamura et al., 1986, 1990; Reinl & Bayerl, 1993; Ter-Minassian-Saraga et al., 1988). Recently, we have come to appreciate that the method provides one of the most sensitive tools to investigate the process of lipid transfer between a single supported bilayer and vesicles. The kinetics of the exchange process can be measured with a time resolution of 10 s, and the amount of lipid transfer can be determined. We employed this method in combination with deuterium NMR and differential scanning calorimetry to study the lipid transfer between a supported bilayer of DMPC and vesicles consisting either of the anionic dimyristoylphosphatidylglycerol (DMPG) or of the cationic lipid analog dioctadecyl diammonium bromide (DODAB).

MATERIALS AND METHODS

Materials. The phospholipids DMPC, DMPG, and their chain perdeuterated analogs DMPC-d_{54} and DMPG-d_{54} were purchased from Avanti Polar Lipids Inc. (Alabaster, AL) and used without further purification. DODAB was obtained from Sigma Chemicals (Deisenhofen, Germany) and was purified by recrystallization. The purity of the lipids used was checked by measuring their respective phase transition temperatures and widths using DSC. Silica beads for the preparation of spherical supported vesicles were obtained as a gift from Dr. Müller from the Degussa Research Laboratories (Degussa AG, Hanau, FRG).

Preparation of Model Membranes. All lipid preparations were done in a 20 mM Hepes buffer at pH 7.0, adjusted with NaOH, and unless otherwise indicated containing 100 mM NaCl.

For multilamellar vesicle (MLV) preparation, the corresponding proportions of dry lipid were weighed into glass test tubes, dissolved in chloroform (5 mg/mL), dried under a stream of nitrogen, and then desiccated overnight in vacuum. The lipid film was then redispersed in buffer at 20 mg/mL and incubated at 50 °C for 30 min with gentle vortexing. For ^{2}H-NMR experiments, deuterium-depleted water was used.

Small unilamellar vesicles (SUV) were obtained by sonicating the MLV suspension with a titanium rod sonifier until an optically transparent vesicle solution with an average vesicle diameter of less than 100 nm (measured by dynamic light scattering) was obtained. The SUV solution was then centrifuged in a tabletop centrifuge to remove titanium dust contamination from the sonifier rod.

Spherical supported vesicles (SSV) were prepared by condensation of small unilamellar vesicles on silica beads of 640 ± 40 nm diameter according to procedures described in detail previously (Bayerl & Bloom, 1990; Naumann et al., 1992).

Single planar bilayer (SPB) of DMPC-d_{54} were obtained by condensation of SUV on a silicon ATR plate inside a home-built FT-IR sample cell described in detail previously (Reinl & Bayerl, 1993). Approximately 1 mL of SUV solution (lipid concentration 10 mg/mL) was transferred into the cell. A circulating external water bath kept the temperature of the cell above the phase transition temperature of the injected SUV solution during the SPB preparation. After a 15-min equilibration of the SUV solution inside the cell, the latter was thoroughly flushed with approximately 100 mL of buffer using a peristaltic pump to remove all SUVs in the bulk solution.

As previously demonstrated by the neutron reflection technique, this procedure provides single bilayers on the solid support (Johnson et al., 1991). Thus, the presence of unstirred layers after a lipid transfer experiment can be excluded.

FT-IR. Infrared spectra were obtained with a Nicolet 60SXR Fourier transform infrared spectrometer equipped with a MCT detector and a vertical attenuated total reflection (ATR) unit. Polarization of the infrared light was achieved by a KRS-5 grid wire polarizer (LOT, Darmstadt, Germany). Depending on the time scale of the exchange kinetics, 15−40 interferograms were collected for each spectrum, at a resolution of 2 cm^{-1}. Data treatment and analysis were performed as previously described (Reinl & Bayerl, 1993). A vertically arranged 52 × 30 × 2 mm, 45° aperture angle silicon crystal was used as ATR element inside the home-built sample cell.

The molar ratio of the supported bilayer constituents was calculated from the ratio of the normalized integral intensities arising from the stretching vibration bands of the CD_2 and CH_2 groups. Normalization was done according to the dipole strength of the corresponding group which was obtained by measuring a equimolar DMPC/DMPC-d_{54} sample over the temperature range of 10−60 °C. This measurement provided a factor of 2.9 ± 0.1 to be applied to the CD_2 intensities in estimating their ratio.

DSC. DSC measurements on spherical supported bilayers were performed with a MC-2 microcalorimeter (Microcal, Amherst, MA) at a scan rate of 30 °C/h (ascending temperature mode only), according to procedures described previously (Naumann et al., 1992). The lipid concentration of the DSC samples was 1.5 mg/mL.

NMR. Deuterium NMR experiments were performed at 61 MHz using a Varian VXR-400S spectrometer equipped with a high power probe. All spectra were obtained using the quadrupolar echo technique with a pulse separation of 20 μs and two 90° pulses of 6 μs duration. The repetition time for successive pulse sequences was 400 ms, and 8 Kb data points were collected with a dwell time of 1 μs. All experiments were done on resonance with a 8 cyclops pulse cycling sequence. An exponential corresponding to a 50 Hz line broadening was applied to the FID signal prior to Fourier transformation. The temperature of the sample was controlled by a Varian temperature control unit and was constant within ±0.2 °C.

RESULTS

Lipid Transfer Kinetics. (a) Zwitterionic Lipid Transfer (DMPC). In the first series of experiments, a single DMPC-d_{54} bilayer on a planar support (silicon ATR crystal) was incubated with 4 mM of sonicated DMPC vesicles (giving a molar ratio DMPC-d_{54}/DMPC $\approx 2 \times 10^{-4}$) at incubation temperatures, $T_{inc} = 25$ and 50 °C (above T_m) and $T_{inc} = 10$ °C (below T_m), where T_m is the phase transition temperature of the phospholipids ($T_m = 24 \pm 0.5$ °C for DMPC, $T_m = 19 \pm 0.5$ °C for DMPC-d_{54}). Owing to the isotopic shift of the methylene stretching vibration frequency of the fatty acyl chains, the signals due to each lipid type can be observed

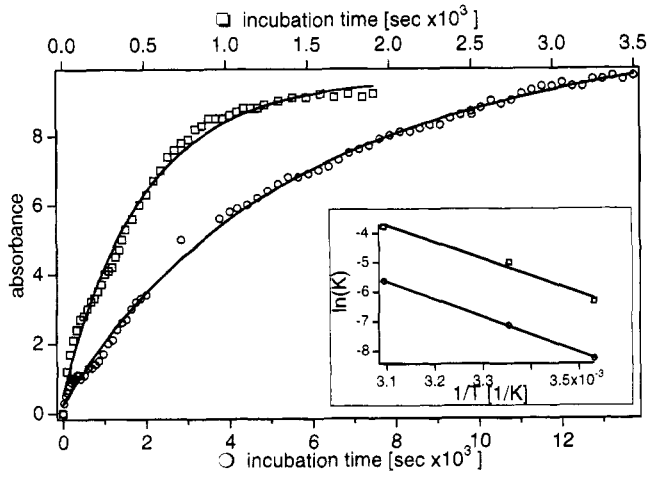

FIGURE 1: Kinetics of the DMPC transfer from sonicated vesicles to a DMPC-d_{54} supported bilayer at an incubation temperature of 10 °C (○) as obtained by measuring the time course of the IR absorbance of the stretching vibration of DMPC (2800−3000 cm^{-1}). The line represents a double exponential fit giving rate constants $K_{2,DMPC} = 8 \times 10^{-5}$ s^{-1} and $K_{1,DMPC} = 2.5 \times 10^{-4}$ s^{-1}. For comparison, the kinetics of the DMPC-d_{54} supported bilayer formation by surface-induced fusion of DMPC-d_{54} sonicated vesicles on the surface of the initially uncoated ATR plate at the same incubation temperature is shown (□). A single exponential fit gives $K_{DMPC\text{-}d54} = 1.8 \times 10^{-3}$ s^{-1}. The insert shows Arrhenius plots of the (initial) rate constants (Table 1) for both DMPC transfer (○) and DMPC-d_{54} supported bilayer formation (□), giving an activation energy of $E_{A,DMPC} = 50 \pm 2$ kJ/mol and of $E_{A,DMPC\text{-}d54} = 48 \pm 2$ kJ/mol, respectively.

Table 1: Lipid Transfer between Sonicated Vesicles of DMPC (Donor) and Supported Bilayer of DMPC-d_{54} (Acceptor) at Various Incubation Temperatures T_{inc}[a]

donor	acceptor	T_{inc} (°C)	K_1 (10^{-4} s^{-1})	K_2 (10^{-4} s^{-1})	R_{eq}
DMPC	DMPC-d_{54}	10	2.5	0.8	2.7
		25	8.0	0.2	1.5
		50	36.0	0.6	2.3

[a] K_1 and K_2 are the fast and the slow rate constants, respectively, obtained by fitting the curves as shown in Figure 1 to double exponentials. R_{eq} represents the ratio of acceptor and donor lipid in the supported bilayer after an incubation time of 4 h. An Arrhenius plot representation of the initial rate K_1 gives an activation energy of $E_{A,DMPC} = 50 \pm 2$ kJ/mol.

simultaneously. Simultaneous with the initiation of the incubation, a time-resolved measurement of the changes in intensity of the above-mentioned signals was started with a time resolution of 30 s, as described in the Materials and Methods section. Plotting the intensity change between consecutive time resolution elements vs incubation time gives the kinetics of the transfer process as shown in Figure 1 for $T_{inc} = 10$ °C. The kinetics data for all three T_{inc} can be fitted to double exponentials (full line in Figure 1), yielding the rate constants given in Table 1. An estimate of the activation energy of the transfer process can be obtained by plotting the initial rate constant $\ln(K_1)$ vs $1/T$ (Arrhenius plot). This gives a straight line (inset in Figure 1) with a slope corresponding to $E_{A,DMPC} = 50 \pm 2$ kJ/mol.

A quantitative assessment of the amount of DMPC transferred to the DMPC-d_{54} bilayer during incubation was obtained by flushing the ATR cell thoroughly with buffer after an incubation time of 4 h. This removes all sonicated vesicles from the cell and enables measurements of the signal intensity arising solely from the supported bilayer. Analysis of the integral intensities of the CH_2 (2800−3000 cm^{-1}) and CD_2 (2000−2300 cm^{-1}) stretching vibrations normalized to the respective transition dipole strengths (cf. Materials and Methods section) gives the composition of the supported bilayer after the DMPC transfer (Table 1). As shown here, the amount of lipid transferred is highest for temperatures near T_m. At 25 °C, we have 39 ± 4 mol % DMPC and 61 ± 4 mol % DMPC-d_{54} after the incubation; the total amount of lipid adsorbed to the ATR plate (obtained as the change in the sum of the CH_2 and CD_2 signal intensities) is constant for all temperatures within an error of 5%. Measurements of the transfer at a lower donor vesicle concentration (2 mM) yields rate constants and R_{eq} (after 4 h incubation), which do not differ significantly from the values in Table 1.

Table 2: Rate Constants K of Bilayer Formation on Silicon ATR Crystal by Surface-Induced Fusion of Sonicated DMPC-d_{54} Vesicles at Various Temperatures, Measured by Time-Resolved FT-IR[a]

T_{inc} (°C)	K (10^{-4} s^{-1})
10	18.0
25	70.0
50	230.0

[a] The K values were obtained by fitting single exponentials to the data as shown in Figure 1.

For comparison, the kinetics of the formation process of a single supported DMPC-d_{54} bilayer on the ATR plate by surface induced fusion of sonicated vesicles at the same temperature and vesicle concentration is also shown in Figure 1. Here, the kinetics was obtained from the time resolved measurement of the CD_2 stretching vibration intensity during the incubation of the (initially uncoated) ATR plate with DMPC-d_{54} sonicated vesicles. The data are shown in Table 2. This kinetics can be fitted by a single exponential and gives a rate constant of $K_{DMPC\text{-}d54} = 1.8 \times 10^{-3}$ s^{-1}. Hence, the formation of the DMPC-d_{54} bilayer exhibits kinetics approximately 1 order of magnitude faster than the transfer of DMPC from sonicated vesicles to the supported bilayer. The activation energy estimated for the bilayer formation process (inset in Figure 1) is $E_{A,DMPC\text{-}d54} = 48 \pm 2$ kJ/mol, very similar to that for the DMPC transfer.

(b) Transfer of Anionic and Cationic Lipids and Lipid Analogs. Figure 2A shows part of the FT-IR spectrum of a DMPC-d_{54} supported bilayer before and after a 2-h incubation with sonicated anionic DMPG vesicles ($T_m = 24 \pm 0.5$ °C) at $T_{inc} = 50$ °C. In each case the measurement was made after flushing the cell. The same donor/acceptor concentration ratio as used in the experiments reported of section (a) was applied here. The incubation with DMPG vesicles causes a drastic drop of the DMPC-d_{54} signal (2000−2300 cm^{-1}) while the DMPG signal (2800−3000 cm^{-1}) grows almost by the same amount. From the integral intensities, we obtain an equilibrium molar ratio of DMPC-d_{54}/DMPG, $R_{eq} \approx 0.34$ in the supported bilayer after the transfer, corresponding to 26% DMPC-d_{54} and 74% DMPG. As in the case of DMPC, the total coverage of the ATR plate with lipid is not significantly altered by the transfer.

In Figure 2B, a similar FT-IR spectrum obtained from a DMPC-d_{54} supported bilayer before and after the incubation with sonicated vesicles of the cationic lipid analog DODAB is presented. All parameters (concentration, incubation time, and temperature) are the same as for the DMPG transfer

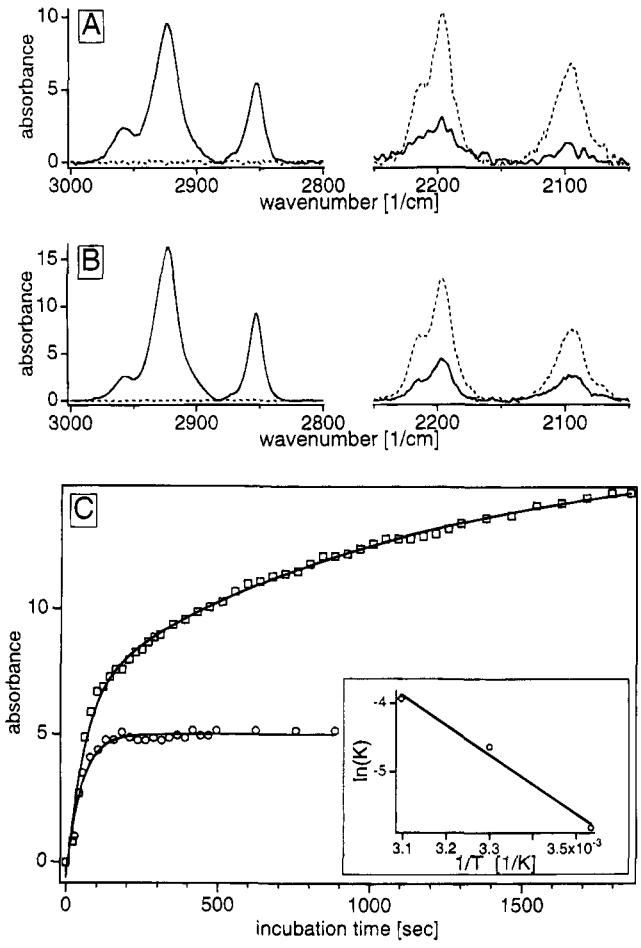

FIGURE 2: (A) FT-IR spectrum of the methylene stretching vibration region of a DMPC-d_{54} single bilayer on a silicon ATR plate before (dotted line) and after (solid line) subjection to lipid exchange with a high excess concentration of sonicated vesicles of DMPG in the bulk. Before the measurement, the ATR cell was thoroughly flushed with buffer in order to prevent any contributions of free vesicles to the signal. Incubation time 2 h; incubation temperature 50 °C. (B) same as A, with DMPG replacing the cationic amphiphile DODAB. (C) Kinetics of the DMPG (○) and DODAB (□) transfers, respectively, to the DMPC-d_{54} supported bilayer at T_{inc} = 50 °C. The full lines represent a fit of the data to a single exponential for DMPG, giving $K_{DMPG} = 19.5 \times 10^{-3}$ s^{-1} and a double exponential for DODAB, giving $K_{1,DODAB} = 16 \times 10^{-3}$ s^{-1} and $K_{2,DODAB} = 9 \times 10^{-4}$ s^{-1}. The inset shows an Arrhenius plot representation of the rate constant ln(K_{DMPG}) (cf. panel C) as a function of the inverse incubation temperature ($1/T_{inc}$), giving an activation energy of $E_{A,DMPG}$ = 35 kJ/mol.

measurement above. The DODAB transfer gives $R_{eq} \approx 0.47$, which corresponds to a composition of the bilayer of 68% DODAB and 32% DMPC-d_{54}. Again, no changes in the total lipid surface coverage were observed.

The kinetics of the DMPG and DODAB transfer, respectively, are represented in Figure 2C. The data for DMPG at T_{inc} = 50 °C can be fitted by a single exponential giving a rate constant $K_{DMPG} = 1.9 \times 10^{-2}$ s^{-1}. In contrast, the DODAB data at this T_{inc} and the DMPG data at lower T_{inc} (30 and 10 °C) require double exponentials for fitting (Table 3). The fast component of the DODAB transfer is similar to that obtained for DMPG and for the deposition of a DMPC-d_{54} bilayer.

Measuring the initial rate constant $K_{1,DMPG}$ at 10, 30, and 50 °C enables the estimation of the activation energy $E_{A,DMPG}$ for the DMPG transfer to the supported bilayer from the slope

Table 3: Lipid Transfer between Sonicated Vesicles of Either DMPG or DODAB (Donor) and Supported Bilayer of DMPC-d_{54} (Acceptor) at Various Incubation Temperatures T_{inc}[a]

donor	acceptor	T_{inc} (°C)	K_1 (10^{-4} s^{-1})	K_2 (10^{-4} s^{-1})	R_{eq}
DMPG	DMPC-d_{54}	10	30.0	3.0	7.3
		30	97.0	10.0	0.38
		50	195.0		0.35
DODAB	DMPC-d_{54}	50	160.0	9.0	0.47

[a] K_1 and K_2 are the fast and the slow rate constants, respectively, obtained by fitting the curves, as shown in Figure 2C, to double exponentials. R_{eq} represents the ratio of acceptor to donor lipid in the supported bilayer after an incubation time of 2 h.

of an Arrhenius plot (inset in Figure 2C), $E_{A,DMPG}$ = 35 ± 2 kJ/mol.

Further salient features of this transfer process can be summarized as follows:

(1) R_{eq} is independent of the excess concentration, c_{ex}, of DMPG or DODAB donor vesicles for $c_{ex} > 2$ mM.

(2) R_{eq} is an equilibrium value at a given temperature and does not depend on the incubation time, provided the latter is longer than the equilibration time.

(3) R_{eq} shows a remarkable dependence on the incubation temperature T_{inc} as shown in Table 1. For values of T_{inc} lower than the chain melting transition temperature of both lipids, a drastic reduction in the amount of DMPG transferred to the supported bilayer is observed.

(4) The incorporation of charged lipids does not result in a significant change of the lipid packing density in the supported bilayer. This is indicated by the unchanged total intensity of the lipid stretching vibration signals.

(5) R_{eq} depends on the ionic strength of the buffer medium. For DMPG, transfer is reduced by more than 1 order of magnitude by doing the transfer in buffer medium without additional NaCl (100 mM for the above experiments). In contrast, DODAB transfer is faster in salt free buffer.

(c) Sequential Transfer of DMPG and DODAB to a DMPC-d_{54} Supported Bilayer. In a second series of measurements the mixed DMPC-d_{54}/DMPG and DMPC-d_{54}/DODAB bilayers that were created by the transfer experiments described in section (b) were incubated with sonicated vesicles of opposite electric charge. The DMPC-d_{54}/DMPG bilayer was now incubated with sonicated DODAB vesicles (case 1), and the DMPC-d_{54}/DODAB bilayer was subjected to DMPG vesicles (case 2). The donor vesicle concentration (4 mM) and the incubation temperature (T_{inc} = 50 °C) were the same as in previous transfer measurements. The incubation results in an increase of the signal corresponding to the CH_2 stretching vibrations of the chains for both cases, as shown in Figure 3. After 2-h incubation and final flushing of the cells, the following compositions of the supported bilayers were measured: case 1: 13 ± 4% DMPC-d_{54} and 87 ± 4% charged lipids; case 2: 16 ± 4% DMPC-d_{54} and 84 ± 4% charged lipids. Hence, from the similarity of the final ratios of charged and zwitterionic lipids in the supported bilayer one might conclude that the sequence of incubation with either DMPG or DODAB has no significant effect on the final composition of the supported bilayer. However, the total amount of lipid adsorbed on the ATR plate differs markedly in the two cases: For case 2 (first DODAB, then DMPG incubation) we obtain a reduction of the total lipid coverage (zwitterionic and charged lipids) by 24 ± 5%. In

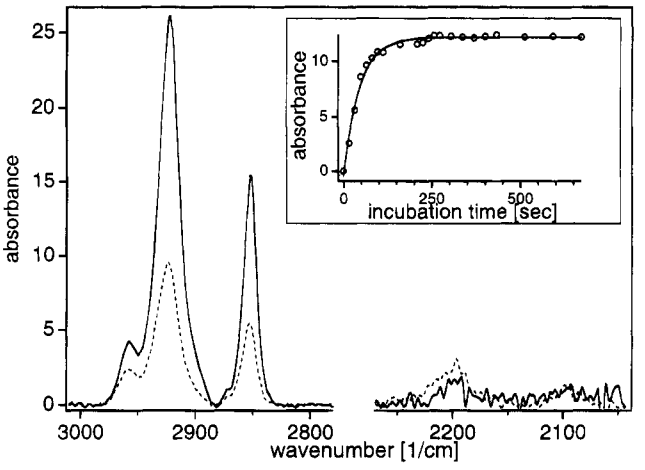

FIGURE 3: FT-IR spectrum (methylene stretching vibration region) of the mixed DMPC-d_{54}/DMPG supported bilayer from Figure 2A (dotted line) and after incubation of the bilayer in the presence of sonicated vesicles of the cationic amphiphile DODAB in the bulk (solid line). Before the measurement, the ATR cell was thoroughly flushed with buffer in order to prevent any contributions of free DODAB vesicles to the signal. Incubation time 2 h, incubation temperature 50 °C. The inset shows the kinetics of the DODAB transfer. Fitting the kinetics to a single exponential gives $K = 23 \times 10^{-3}$ s^{-1}.

contrast, case 1 (first DMPG, then DODAB incubation) exhibits a significant increase of the lipid coverage by 35 ± 5%.

Further insight about the ratio of the charged lipids in the bilayer can be obtained from intensity changes in the C=O stretching vibration (1740 cm^{-1}), since the DODAB does not exhibit such a band while DMPG (and DMPC) do. For case 2 (first DODAB, then DMPG), the C=O signal exhibits a decrease in intensity due to the incubation with DMPG vesicles which is proportional to the reduction of the CD_2 signal. This indicates an approximately 1:1 exchange of DMPG with DMPC-d_{54}. In contrast, case 1 shows no significant reduction of the C=O signal intensity despite the above-mentioned drastic increase of the total bilayer coverage, indicating that the incubation with DODAB vesicles causes essentially a net transfer of DODAB to the supported bilayer.

The transfer kinetics in both case 1 and case 2 can be fitted by a single exponential, yielding rate constants of $K^*_{DODAB} = 23 \times 10^{-3}$ s^{-1} and of $K^*_{DMPG} = 9.7 \times 10^{-3}$ s^{-1}, respectively.

The final surface charge of the supported bilayer formed by case 1 and case 2 can be probed by filling the ATR cell again with either DMPG or DODAB multilamellar vesicles at $T_{inc} = 10$ °C and low ionic strength (1 mM NaCl) on observing changes of the CH_2 vibration signal intensity. The low T_{inc} is used to keep lipid transfer negligible, since all lipid components are in the gel phase state at 10 °C, and the low NaCl concentration reduces the screening of the electrostatic potential. Since the penetration depth of the evanescent IR field is ≈0.5 μm for our setup, the signal results not only from the lipids in the supported bilayer, but also from those in vesicles close to the bilayer.

For the bilayer resulting from case 1 (first DMPG, then DODAB), incubation of the bilayer with DMPG vesicles does not cause any significant increase of the signal intensity in the 2800−3000 cm^{-1} range. The surface charge of the bilayer prevents DMPG vesicles from coming close enough

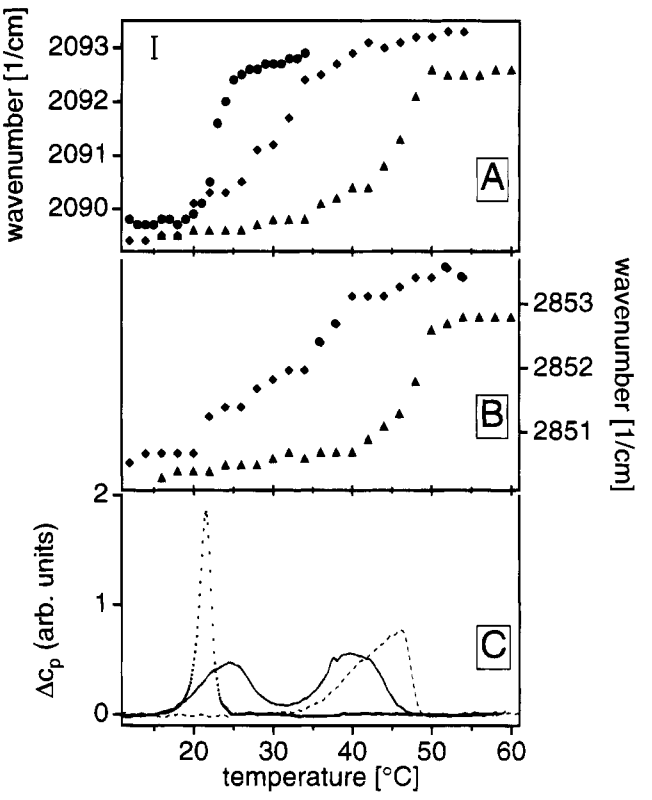

FIGURE 4: (A) Temperature dependence of the IR symmetric CD_2 stretching vibration frequency of DMPC-d_{54} in a supported bilayer at the three stages of the lipid exchange experiment from Figure 2 pure DMPC-d_{54} bilayer prior to the incubation with vesicles (●), mixed DMPC-d_{54}/DODAB bilayer (♦), and the ternary mixed bilayer DMPC-d_{54}/DODAB/DMPG (▲). The measurements were done after the bilayer assumed its equilibrium composition R_{eq} and the remaining bulk vesicles had been removed by flushing the cell with buffer. The error bar is representative for the frequency determination error for all temperatures. (B) Same as A, but for the CH_2 stretching vibration frequency arising after the incubation of the bilayer with DODAB (♦) and with DMPG (▲). (C) DSC endotherms of a spherically supported bilayer of pure DMPC-d_{54} (dotted), after the incubation with DODAB (solid line) and finally with DMPG (dashed), analogous to the FT-IR measurements in panels A and B. Silica beads of 640 ± 40 nm diameter were used as a spherical support. The sonicated vesicles in the bulk used in the lipid exchange were removed prior to the measurement.

to the membrane to be detectable in the evanescent field. In contrast, incubation with the same concentration of DODAB vesicles drastically increases the signal intensity by an order of magnitude. This clearly indicates that the net surface charge of the mixed bilayer is negative, so that the positively charged DODAB vesicles couple to it by Coulomb interaction.

For case 2 (first DODAB, then DMPG) the opposite behavior was observed, indicating that the case 2 bilayer exhibits a positive net surface charge.

Phase Transition Behavior of Supported Bilayer. Observing changes of the phase transition of the supported bilayer in the course of lipid exchange or lipid transfer can help to distinguish between the incorporation of lipids into the bilayer and the mere adsorption of vesicles to it. Figure 4A shows the temperature dependence of the symmetric CD_2 stretching vibration frequency of the DMPC-d_{54} at the three phases of the case 2 experiment: pure DMPC-d_{54} bilayer prior to the incubation with vesicles, mixed DMPC-d_{54}/DODAB bilayer, and the ternary mixed bilayer DMPC-d_{54}/

DODAB/DMPG, each of the latter two measured after reaching their R_{eq} and the removal of the remaining bulk vesicles by flushing the cell with buffer. Figure 4B shows the same for the signal arising from the nondeuterated bilayer constituents (DODAB and DMPG). All curves exhibit the well known sigmoid shape typical for a chain melting transition. Noteworthy details are: The DODAB causes a significant broadening to the DMPC-d_{54} phase transition while the final incubation with DMPG narrows the transition again but shifts it by 10−15 °C toward higher temperature.

A similar feature can be observed for the electrically charged species (Figure 4B): DODAB exhibits a broad transition between 20 and 45 °C (pure DODAB has a rather sharp phase transition at T_m = 48 °C) and the incubation with DMPG (T_m = 24 °C for pure DMPG) renders the transition narrower and shifts it to a similar temperature range as observed for the DMPC-d_{54} in the ternary mixture.

Differential scanning calorimetry (DSC) can also be used to measure the phase transition of a supported bilayer as shown previously (Naumann et al., 1992). Spherical silica beads (diameter 640 ± 40 nm) are used as a solid support. It should be emphasized that such spherically supported single bilayers are in fact (with the obvious exception of the curvature) a completely analogous system to the planar supported bilayer used for the FT-IR: In both systems the single bilayer faces a negatively charged SiO_2 surface. Figure 4C shows three DSC endotherms of a spherically supported DMPC-d_{54} bilayer at the three stages of the lipid exchange/transfer as in Figure 4A,B. The sonicated vesicles in the bulk used for the lipid transfer were removed prior to the DSC measurements. Generally, the results agree well with those obtained by the FT-IR measurements. However, the DSC shows more clearly that incubation with DODAB not only broadens the transition significantly, but causes a demixing of the bilayer in the gel phase. A similar endotherm is observed for a multilamellar dispersion of DMPC with 15 mol % DODAB (T. M. Bayerl, unpublished results). Comparison with the FT-IR results shows that the DSC peak around 24 °C is caused mainly by the melting of DMPC-d_{54} while the peak at 39 °C arises from the melting of a domain containing high proportions of DODAB. For the final state of the supported bilayer, i.e., after the incubation with DMPG, both DSC and FT-IR show the T_m shift toward higher temperatures but no demixing is indicated.

Changes of Molecular Order and Dynamics. The above mentioned drastic increase of the bilayer packing density owing to the sequential transfer of DMPG and DODAB (case 1) by about 35% suggests that the DODAB transfer might result in the formation of an asymmetric supported bilayer. The deuterium NMR line shape can be sensitive to such asymmetries provided the two leaflets have different molecular order, and the exchange between them is slow on the NMR time scale. Therefore, deuterium NMR measurements were performed employing chain perdeuterated DMPG-d_{54} on a supported DMPC bilayer on spherical silica beads after the sequential transfer of DMPG and DODAB, respectively (T_{inc} = 50 °C). In Figure 5A, the spectrum of the DMPG-d_{54} after being transferred to the supported DMPC bilayer is shown. The line shape of this spectrum and its quadrupolar splitting of the edges ($\Delta\nu_Q$ = 24.1 kHz) is very similar to that obtained for a pure DMPC-d_{54} sample under

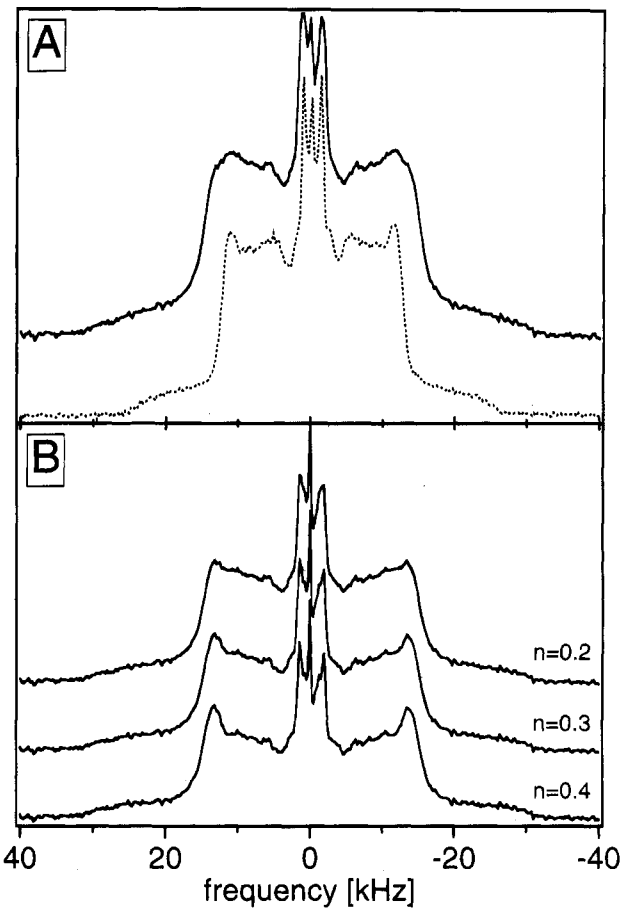

FIGURE 5: (A) Deuterium NMR spectra of a single bilayer on a spherical support of silica beads (diameter 640 ± 40 nm) after incubation of a pure DMPC bilayer with DMPG-d_{54} sonicated vesicles at 50 °C for 2 h and the removal of the bulk vesicles by washing the sample (dotted line). The full line spectrum was obtained after incubating the sample again, but with sonicated DODAB vesicles under otherwise identical conditions. (B) Deuterium NMR spectra obtained after a spectral subtraction of the two spectra from panel A using different weights n between the two spectra (see text for details).

the same conditions (spectrum not shown). Hence, the transfer of DMPG-d_{54} to the supported bilayer does not result in measurable changes of molecular order in the bilayer.

An interesting feature of Figure 5A is the absence of any significant isotropic signal. This is clear evidence that all transferred DMPG-d_{54} must be located in the supported bilayer since any signal arising from DMPG-d_{54} in small vesicles like those used for the incubation must give an isotropic line shape owing to motional averaging on the NMR time scale.

The second spectrum in Figure 5A was obtained after incubation of the DMPC/DMPG-d_{54} sample with DODAB vesicles under the same conditions as for the FT-IR experiments. It is obvious that the DODAB causes a significant increase of the quadrupolar splitting of the spectrum by $\Delta(\Delta\nu_Q)$ = 5 kHz, indicating an increase of the molecular order parameter of the DMPG-d_{54} chains. Moreover, there is a remarkable "rounding" effect of the edges of the spectrum (corresponding to the 90° orientation of the molecular director with respect to the external field) together with a broadening of the terminal methyl group signal at ±1.4 kHz. This odd line shape strongly suggests that the spectrum represents a superposition of two pake doublets with different

quadrupolar splitting. Asssuming that one spectral component of the superposition is represented by the line shape $I_1(\omega)$ of the DMPC/DMPG-d_{54} spectrum from Figure 4A, the second component $I_2(\omega)$ can be obtained according to $I_2(\omega) = I_{tot}(\omega) - nI_1(\omega)$ where $I_{tot}(\omega)$ is the line shape of the composite spectrum (DMPC/DMPG-d_{54}/DODAB) and n is a normalization constant between 0 and 1. Figure 5B shows the result for such a subtraction for three representative values of n. The correct value of n can now be identified by assuming that the order parameter distribution function is similar for both $I_1(\omega)$ and $I_2(\omega)$. This would indicate $n \approx 0.3$ and a quadrupolar splitting of $\Delta\nu_Q = 27$ kHz. A more direct approach is the comparison with a spectrum obtained at the same temperature for a multilamellar dispersion of the three components at a molar ratio as determined by the above IR measurements. Unfortunately, multilamellar dispersions of this mixture are prone to significant macroscopic orientation effects at the magnetic field strength used for the NMR measurements (9.6 T) (cf. Brumm et al. (1992)). This renders the line shape incomparable to that of the (nonorienting) supported system. The only parameter which remains comparable is the quadrupolar splitting of the edges which is $\Delta\nu_Q = 27.5$ kHz for the multilamellar dispersion (data not shown) in good agreement with the $\Delta\nu_Q$ obtained by the subtraction technique (Figure 5B). Hence, the NMR data indicate that owing to the DODAB uptake, the DMPG-d_{54} distributes with a 7:3 stoichiometry between two regions of the supported bilayer characterized by different molecular order. Moreover, the exchange between the two regions must be slow on the NMR time scale.

DISCUSSION

The results obtained can be summarized as follows:

(1) Measurements of supported bilayers by infrared ATR technique enables a sensitive assessment of lipid exchange between the supported bilayer and small sonicated vesicles in bulk.

(2) A single DMPC-d_{54} bilayer on a solid support can be modified with regard to their lipid composition and surface charge by a spontaneous transfer of lipids between small sonicated vesicles and a supported bilayer.

(3) Transfer of either anionic DMPG or cationic DODAB to the supported DMPC-d_{54} bilayer does not cause significant changes in the lipid packing density of the bilayer. For DMPG transfer, the activation energy of $E_{A,DMPG} = 35 \pm 2$ kJ/mol was estimated while E_A for DMPC transfer is significantly higher ($E_{A,DMPC} = 50 \pm 2$ kJ/mol). The equilibrium composition of the supported bilayer due to the transfer is rather independent of cationic or anionic species being transferred.

(4) The DMPC-d_{54} in the supported bilayer cannot be replaced completely by lipids from sonicated vesicles despite large excess concentrations of the latter and of incubation times of several hours. This finding is independent of the charge characteristics of transferred lipid and holds for DMPC also.

(5) Sequential subjection of the DMPC-d_{54} bilayer to transfer with both DODAB and DMPG gives a supported bilayer containing all three species where the ratio between DMPC-d_{54} and the charged species is independent of sequence, i.e., whether first DMPG or DODAB is being transferred. In contrast, the final lipid packing density of the supported bilayer was found to be drastically dependent on the sequence.

(6) All lipid transfers cause changes in the phase transition behavior of the supported bilayer.

(7) ^{2}H-NMR on a supported bilayer, containing all three species and created by a sequential transfer of DMPG-d_{54} and of DODAB, indicates that the DMPG-d_{54} is partitioned between two environments of the supported bilayer with different molecular order and with an exchange rate which is slow on the NMR time scale. The stoichiometry of the DMPG-d_{54} between the two species was estimated to be approximately 2:1. Moreover, the NMR results evidence that all lipids transferred are inserted in the supported bilayer.

Asymmetric Lipid Distribution. One of the most intriguing questions is whether the mixed supported bilayer exhibits an inhomogeneous distribution of the charged species between the inner and the outer leaflet owing to the negative surface charge of the solid support. A conceivable arrangement would be the enrichment of cationic species in the leaflet facing the solid support while the outer leaflet would exhibit increased amounts of anionic DMPG. The driving force for such a transversal demixing would be the difference in electrostatic pressure between the solid surface and the anionic charges in the inner and the outer monolayer, respectively. This pressure difference can be estimated from the DLVO theorie to be $\Delta P \approx 3 \times 10^5$ Nm^{-2} for a bilayer separated by a 15 Å water gap from the silicon surface. In order to keep the distribution of the charged species homogeneous, the difference in chemical potential $\Delta\mu$ between the two leaflets owing to the asymmetry must compensate ΔP.

Our results give no indication that an asymmetry is caused by the presence of either DMPG or DODAB alone in the DMPC-d_{54} bilayer under conditions of 100 mM NaCl in the buffer. However, the sequential transfer of DMPG and DODAB (case 1) to the supported bilayer seems to induce an asymmetry. This is indicated by two findings. One is the NMR result for case 1, which strongly suggests that the DMPG is partitioned between two environments with significantly different molecular order. The formation of domains in the supported bilayer is an unlikely explanation for the observed line shape (Figure 5A) since the measurements were performed in the liquid crystalline phase state. There the lateral diffusion of the lipid is always sufficiently fast on the NMR time scale to average out a possible quadrupolar splitting difference for DMPG-d_{54} partitioned in domains which are enriched or depleted of DODAB. An asymmetric distribution of DODAB between the two monolayers is the most likely explanation for the observed line shape since transbilayer lipid exchange (flip-flop) is certainly a process which is slow on the NMR time scale (microsecond range). In our simple subtraction procedure (Figure 5B) the assumption was made that the monolayer facing the silica surface does not take up significant amounts of the DODAB so that the quadrupolar splitting of DMPG-d_{54} partitioned there does not change. Under this assumption, we can assign 30% DMPG-d_{54} to the inner monolayer and 70% to the outer one as deduced from the factor $n = 0.3$ used for the subtraction. The DODAB in the outer monolayer can be expected to form high melting complexes with the DMPG owing to the attractive electrostatic potential between them (Silvius, 1991), as experimentally observed by DSC and FT-IR (Figure 4). Such complexes enable a high packing density

of the lipids involved, which may explain the observed increase in the total lipid coverage of the surface by 35%. The finding that the DODAB transfer in case 1 is essentially a net transfer (neither DMPG nor DMPC-d_{54} are depleted in the bilayer due to the transfer) provides additional support for the assumption of an asymmetric lipid distribution.

Further support for the existence of an asymmetry comes from the different net surface charge of the mixed supported bilayer, depending on the sequence of the incubation with DODAB or DMPG. The results indicate that the charged lipid species being transferred first in the sequence to the DMPC-d_{54} supported bilayer determines its net surface charge. For the case 1 experiment (DMPG first, DODAB second) this makes sense since the bilayer contains already 74% DMPG before the DODAB incubation and the latter does not remove any DMPG or DMPC-d_{54} from the bilayer.

There are two likely explanations for the enrichment of DODAB in the outer monolayer. The formation of complexes with DMPG in the outer monolayer could drastically reduce the flip-flop of the complexed species owing to a high activation energy. Moreover, the formation of complexes may reduce the chemical potential difference between the two monolayers which is an essential driving force for flip-flop in planar bilayers. The counterion concentration [Na^+] in the water gap between the bilayer and the ATR plate may be a second important obstacle to DODAB transfer to the inner monolayer. The counterion concentration must be sufficiently high to screen the repulsive electrostatic potential completely between the ATR plate and the bilayer containing 74% DMPG. The entry of DODAB into the inner monolayer via flip-flop would consequently require a partial exchange of Na^+ in the gap by Cl^-. This could be achieved only by ion permeation across the bilayer. Hence, this energetically unfavorable process may slow down or prevent the equilibration of DODAB between the monolayers.

Lipid Transfer Mechanism. Three potential lipid transfer mechanisms may contribute to lipid transfer between sonicated vesicles and a supported bilayer. Monomeric transfer, enhanced monomeric transfer by transient close opposition of vesicles and supported bilayer and (transient) fusion of vesicles with the bilayer.

Lipid transfer by enhanced monomer desorption from the donor vesicles due to a transient, collision-controlled, close opposition of donor and acceptor bilayers was recently suggested as a second order type transfer mechanism dominating at high lipid concentrations (>2 mM) (Jones & Thompson, 1989, 1990). This mechanism predicts a concentration dependence of the kinetics on the acceptor concentration. Since the acceptor concentration in our experiments is low (2×10^{-3} mg lipid on the ATR plate compared to 10 mg vesicles in the bulk), second order transfer effects arising from direct collisions between vesicles and the supported bilayer are presumably negligible.

Monomeric lipid transfer, which is generally recognized to be independent of vesicle concentration owing to the rate limiting monomer desorption from the donor vesicles, could be a likely mechanism since we observed a concentration independence of the transfer kinetics. Therefore, it is interesting to compare our activation energy for the DMPC transfer ($E_{A,DMPC}$ = 50 kJ/mol) with those obtained by other methods. Using tritium labeled DMPC, Wimley and Thompson (1990) obtained $E_{A,DMPC}$ = 104 kJ/mol for the transfer between large unilamellar vesicles in the L_α state. For sonicated vesicles they estimated $E_{A,DMPC}$ = 83 kJ/mol for the L_α phase using data from (McLean & Phillips, 1984). Thus, the activation energy we obtain for transfer between sonicated vesicles and a supported bilayer is approximately 40% lower than for monomeric transfer between sonicated vesicles. Assuming that the activation energy is mainly determined by the desorption of the lipid monomers from the donor vesicles, one would expect no difference in the E_A values for different acceptors (vesicle or supported bilayer). Hence, monomeric lipid transfer is unlikely to be the dominating mechanism in our experiments.

Temporary vesicle fusion has been suggested as a possible lipid transfer mechanism (Brown, 1992), and our E_A value obtained for DMPC transfer is similar to that obtained from bilayer formation, but some kinetic differences in the bilayer formation by vesicle fusion remain: The DMPC transfer rate is 1 order of magnitude lower than that obtained for the DMPC-d_{54} supported bilayer formation. It is widely acknowledged that the latter process is achieved by the collapse and subsequent fusion of the sonicated vesicles onto the solid surface (Iler, 1979; McConnell et al., 1986; Czaja et al., 1987). Moreover, the kinetics of the bilayer formation can be described by a single exponential fit while two exponentials are required for the DMPC transfer.

In spite of these differences, we interpret our data in terms of the transient fusion model owing to collisions between the vesicles and the supported bilayer. This model, although rarely applied for the description of transfer between vesicles, seems most appropriate considering that the supported bilayer represents a perfectly hard wall for collisions with vesicles. Since the kinetic energy of a vesicle colliding normal to the supported bilayer must be dissipated, close contact with the supported bilayer and a (temporary) collapse of the vesicle on top of it are very likely. It should be emphasized that this situation is different from collisions between vesicles, where most of the kinetic energy is simply transferred between them and thus rarely giving rise to a fusion. The similar activation energy obtained for DMPC transfer and for bilayer formation by surface induced vesicle fusion strongly supports our assumption. Further support comes from the finding that transfer takes place even at temperatures where both donor and acceptor are in the gel phase. Desorption of DMPC-d_{54} from the supported bilayer (exchange with DMPC) requires an activation energy well above 100 kJ/mol. Inelastic collisions of vesicles with the supported bilayer can cause a local melting of both donor and acceptor, which may provide such energies.

The differences in the kinetics of the two processes can be explained by appreciating that a transfer of DMPC from the vesicles to the DMPC-d_{54} supported bilayer is a two step transport process. It requires, in contrast to bilayer formation, the removal of an appropriate amount of DMPC-d_{54} from the bilayer prior to the uptake of donor lipid (DMPC). This renders the transfer less efficient compared to bilayer formation where lipids can (initially) spread out on the solid surface without such restraints.

A rational for the biexponentiality of transfer kinetics observed at lower temperatures is not given here. However, it is unlikely that very small unilamellar vesicles that may be present in the sonicated vesicles dispersion can account for this behavior. This is because such vesicles are extremely unstable and tend to fuse rapidly to larger ones upon crossing the phase transition (Lentz et al., 1987).

Effects of Charge State of Vesicles on Lipid Transfer. The surface charge of the solid support is expected to influence the charge selectivity of lipid transfer. We observe this for low ionic strength which causes a drastic slowdown of DMPG transfer to the supported bilayer, while DODAB transfer was accelerated at 1 mM NaCl. This finding is in contrast to measurements of DMPG transfer between vesicles where an acceleration of the DMPG transfer at low ionic strength was observed (Jones & Thompson, 1990). This different behaviour stresses the importance of the solid support surface charge for the transfer at low salt concentrations. However, most of our measurements were done with 100 mM NaCl in the buffer medium, which reduces the Debye length to ≈10 Å. This explains why no signifcant selectivity of the sign of the headgroup charge with respect to the amount of charged lipid transferred to the supported bilayer was observed.

The amount of DMPC-d_{54} in the supported bilayer which is inaccessible to exchange with charged lipids (cf. Table 3) is another interesting point. Since this amount is well below 50% of the total lipid content, it does not indicate intrabilayer asymmetry owing to a hindrance of flip-flop between the two monolayers. A more likely reason is the presence of Na^+ and Cl^- ions in the water gap between the bilayer and the ATR plate. The change of the electrostatic potential between the bilayer and the ATR plate in the course of the transfer of charged lipids would require a redistribution of ions in order to keep the bilayer stable. Such a redistribution could be achieved only by ion permeation through the bilayer, which is a rather slow process.

A comparison of the transfer kinetics for DMPC (Table 1) and for the charged lipids (Table 3) reveals drastic differences. Transfer of charged lipids to the supported bilayer is an order of magnitude faster and can be described by a single exponential fit to the data (at T_{inc} = 50 °C). In terms of the transient fusion model discussed above this would indicate that charged vesicles exhibit a higher fusion efficiency with the supported DMPC-d_{54} bilayer. This can be attributed to (i) the significantly higher chemical potential difference between the charged vesicles and the DMPC-d_{54} supported bilayer (compared to DMPC donor vesicles) and to (ii) the higher curvature of the charged vesicles, which renders them less stable during collisions with the bilayer. For the DMPC transfer the difference in chemical potential arises mainly from the curvature of the vesicles compared to the planar supported bilayer (assuming that the isotope effect is negligible). In contrast, the charged lipids give additional contributions to the chemical potential owing to their headgroup charge and their structural differences.

CONCLUSIONS

The formation of stable, asymmetric lipid bilayers on a solid support via lipid transfer from sonicated vesicles shows that lipid asymmetries, which are well-established for biological systems (e.g., erythrocytes), can be created by a self-assembly process in model systems as well. While in biological systems active transport by proteins is assumed to be the driving force for the asymmetry, intermolecular forces determine the asymmetry in supported bilayers. This feature of supported bilayers could be interesting for future studies of the effect of lipid asymmetry on the interaction of bilayers with water soluble proteins.

REFERENCES

Bayerl, T. M., & Bloom, M. (1990) *Biophys. J. 58*, 357.

Bayerl, T. M., Schmidt, C. F., & Sackmann, E. (1988) *Biochemistry 27*, 6078.

Brown, R. E. (1992) *Biochim. Biophys. Acta 1113*, 375.

Brumm, T., Möps, A., Dolainsky, C., Brückner, S., & Bayerl, T. M. (1992) *Biophys. J. 61*, 1018.

Czaja, C., Jekutsch, G., Rothenhäusler, B., & Gaub, H. E. (1987) *Biosensors 3*.

Dolainsky, C., Möps, A., & Bayerl, T. M. (1993) *J. Chem. Phys. 98*, 1712.

Frey, S., & Tamm, L. K. (1991) *Biophys. J. 60*, 922.

Iler, R. K. (1979) *The chemistry of silica*, Wiley & Sons, New York.

Johnson, S. J., Bayerl, T. M., McDermott, D. C., Adam, G. W., Rennie, A. R., Thomas, R. K., & Sackmann, E. (1991) *Biophys. J. 59*, 289.

Jones, J. D., & Thompson, T. E. (1989) *Biochemistry 28*, 129.

Jones, J. D., & Thompson, T. E. (1990) *Biochemistry 29*, 1593.

Köchy, T., & Bayerl, T. M. (1993) *Phys. Rev. E47*, 2109.

Lentz, B. R., Carpenter, T. J., & Alford, D. R. (1987) *Biochemistry 26*, 5389.

McConnell, H. M., Watts, T. M., Weiss, R. M., & Brian, A. A. (1986) *Biochim. Biophys. Acta 864*, 95.

McLean, L. R., & Phillips, M. C. (1984) *Biochemistry 23*, 4624.

Naumann, C., Brumm, T., & Bayerl, T. M. (1992) *Biophys. J. 63*, 1314.

Okamura, E., Umemura, J., & Takenaka, T. (1986) *Biochim. Biophys. Acta 856*, 68.

Okamura, E., Umemura, J., & Takenaka, T. (1990) *Biochim. Biophys. Acta 1025*, 94.

Reinl, H. M., & Bayerl, T. M. (1993) *Biochim. Biophys. Acta 1151*, 127.

Silvius, J. R. (1991) *Biochim. Biophys. Acta 1070*, 51.

Tamm, L. K., & McConnell, M. (1985) *Biophys. J. 47*, 105.

Tamm, L. K., & Tatulian, S. A. (1993) *Biochemistry 32*, 7720.

Ter-Minassian-Saraga, L., Okamura, E., Umemura, J., & Takenaka, T. (1988) *Biochim. Biophys. Acta 946*, 417.

Thompson, N. L., & Palmer, A. G. (1988) *Comm 5*, 39.

Wimley, W. C., & Thompson, T. E. (1990) *Biochemistry 29*, 1296.

Wimley, W. C., & Thompson, T. E (1991) *Biochemistry 30*, 4200.